Journal of Applied Polymer Science

In Situ Polymerized Nanocomposites of Poly(butylene succinate)/TiO_2 Nanofibers: Molecular Weight, Morphology, and Thermal Properties

Weidong Zhou, Tao Xu, Xiaowei Wang, Erjuan Zhi, Jun Liu, Wei Zhang, Junhui Ji
Technical Institute of Physics and Chemistry, Chinese Academy of Science, Beijing 100190, China
Correspondence to: J. Ji (E-mail: jijunhuichina@gmail.com)

ABSTRACT: In this study, the nanocomposites of poly(butylene succinate) (PBS) and TiO_2 nanofibers were first synthesized via *in situ* polymerization. Molecular weight, morphology, and thermal properties of the nanocomposites were characterized. As the weight percentage of TiO_2 nanofibers increased from 0 to 2%, the molecular weight of PBS in the nanocomposites decreased gradually compared with that of pure PBS. In morphology, the nanocomposites were constituted by free PBS and PBS-grafted TiO_2 nanofibers (PBS-*g*-TiO_2), which were proved by the Fourier transform infrared, scanning electron microscopy (SEM), and transmission electron microscopy. In addition, the SEM demonstrated the strong interfacial interaction and homogeneous distribution between TiO_2 nanofibers and PBS matrix. The thermal properties determined by differential scanning calorimetry and thermogravimetric analysis included the increasing of cold crystallization temperatures, the melting temperatures, and the thermal stability. Besides, the crystallinity and the rate of crystallization of the nanocomposites were enhanced, which were also observed by the X-ray diffraction.

KEYWORDS: poly(butylene succinate); TiO_2 nanofibers; molecular weight; morphology; thermal properties

Received 29 November 2011; accepted 18 March 2012; published online
DOI: 10.1002/app.37724

INTRODUCTION

In last few years, the rapid growth of plastics has caused many environmental problems that attract great attention to the biodegradable plastics. Recently, their development was further promoted by the rising petroleum price and expanding ecological pollution. During this period, many commercial biodegradable polymers are studied, such as poly(butylene succinate) (PBS), poly(lactic acid) (PLA), poly(hydroxyvalerate)s (PHAs), etc. Among these, PBS synthesized by succinic acid (Su) and 1,4-butanediol (Bu) has shown excellent thermoplastic processability and balanced mechanical properties, which is recognized as one of the most promising biodegradable plastics.[1] However, the low melt viscosity, poor impact strength, and slow crystallization rate limit its application in the field of film, foam, and injection molding products. Moreover, its uncontrollable degradation performance is also an obvious shortcoming.[2] Lately, many efforts have been done to modify the properties of PBS to meet the different requirements, among which the introduction of inorganic nanofillers is an effective way. The nanofillers such as silica, silicate, montmorillonites, organoclay, carbon nanotube, graphene, etc. have remarkable influences on the thermal stability, mechanical, rheological, and biodegradable properties of PBS nanocomposites.[3–8]

With the high photocatalytic activity, TiO_2 nanopowders have been widely used to treat waste water, clean indoor air, hydrophilic self-cleaning, antibacterial, etc.[9,10] The adding of TiO_2 into both nonbiodegradable and biodegradable polymers can obviously improve thermal-mechanical properties and speed up their degradation under sunlight.[11–14] However, the surface treatment of TiO_2 is necessary to improve the compatibility and dispersion in polymer matrix that limits its wide application. In recent researches, TiO_2 nanofibers could be synthesized by several different methods.[15–18] With large quantities of hydroxyl groups on surface, TiO_2 nanofibers can more easily form network structures through direct interaction and chains grafting to the polymer matrix.[19] The grafted reactions between TiO_2 and polymers had been found in TiO_2/poly(acrylic acid), TiO_2/PLA, etc.[20–22] Hence, we believe that TiO_2 nanofibers can play a meaningful role in regulating the crystallization, thermal-mechanical, and biodegradable properties of PBS compared with conventional nanopowders.

It is difficult to synthesize polymer nanocomposites with targeted properties. The reason lies in the fact that nanofillers will typically agglomerate due to their hydrophilic nature and high surface area, and they will not be miscible with hydrophobic polymer phase.[23,24] To solve this problem and enhance the

interaction between nanofillers and PBS, we dispersed TiO_2 nanofibers into hydrophilic Bu with the aid of ultrasonic treatment and intense mechanical stirring. In this article, (1) we first succeeded in synthesizing the TiO_2 nanofibers and the PBS/TiO_2 nanocomposites. Such nanocomposites have achieved nanoscale homogeneous dispersion and strong interfacial interaction between TiO_2 and PBS matrix. (2) Besides, we further proved the existence of PBS-grafted TiO_2 nanofibers (PBS-*g*-TiO_2) nanofibers by the chemical structure and morphology analysis of the isolated PBS-*g*-TiO_2. (3) And we further characterized the molecular weight, morphology, and thermal properties of the nanocomposites to study the influence of TiO_2 nanofibers and the grafted structure.

EXPERIMENTAL

Materials

Su (≥99%), Bu (≥98%), and titanium butoxide (TBT, ≥ 99%) were obtained from Aladdin Reagent (Shanghai, China) and used as received. TiO_2 nanopowders (ST-01) were purchased from Ishihara Sangyo Kaisha (Japan). Sodium hydroxide (NaOH) and the other materials and solvents were provided by Sinopharm Chemical Reagent (Shanghai, China).

TiO_2 Nanofibers, PBS/TiO_2, and PBS-*g*-TiO_2 Preparation

To get the TiO_2 nanofibers, we followed a simple chemical approach described by Yang et al.[25] TiO_2 (6 g) nanopowders was mixed with 80 mL of 10*M* NaOH. Then the slurry was transfered into an autoclave with a PTFE container inside to be heated in a muffle with the temperature at 180°C for 48 h. After that, the precipitate was washed with deionized water until the pH reached 7. At the last, the produced TiO_2 nanofibers were dried at 80°C for 24 h.

To synthesize the PBS/TiO_2, TiO_2 nanofibers were added gradually to Bu and ultrasonically treated for 30 min to ensure the uniform dispersion. Then the Su and TBT were added with mol ratio of 1 : 0.0002. The mixture was dehydrated at 180°C under nitrogen for 2 h with mechanical stirring. Then the polycondensation was done at 220°C under a reduced pressure of 10 Torr for 6 h. According to the weight percentage of TiO_2, they were labeled as PBS/0.5%TiO_2, PBS/1%TiO_2, and PBS/2%TiO_2. Pure PBS without TiO_2 was prepared following the same procedures and used as a control.

Table I. Molecular Weight of PBS and PBS/TiO2 Determined by GPC Measurement

Samples	M_n	M_w	PDI
PBS	42,300	73,700	1.7
PBS/0.5% TiO_2	31,600	58,800	1.9
PBS/1% TiO_2	27,300	57,300	2.1
PBS/2% TiO_2	20,500	45,100	2.2

To separate the PBS-*g*-TiO_2 from free PBS, we used a repeated dispersion/centrifugation process following the other literature.[26] Briefly, we dispersed a portion of PBS/2%TiO_2 in chloroform and the solution was centrifugated at 8500 rpm for 30 min. The operation was performed repeatedly five times to ensure physically absorbed free polymers were completely removed. At last, the PBS-*g*-TiO_2 was dried in a vacuum oven at 80°C for 24 h.

Measurements

The X-ray diffraction (XRD) patterns were recorded on a Bruker D8 focus, using Cu-Kα radiation set at a voltage of 40 kV and a current of 40 mA. The scans ranged from 5 to 60°, with a scanning rate of 6°/min.

Fourier transform infrared (FTIR) spectra were acquired with an Excalibur 3100. Spectra were collected in the region of 4000–500 cm^{-1} with a spectral resolution of 4 cm^{-1} and 32 scans co-added.

The weight average molecular (M_w), number average molecular (M_n), and molecular weight distribution (PDI = M_w/M_n) were determined through Gel permeation chromatography (GPC). Samples were dissolved in chloroform and all the solutions were filtered with 0.2 μm Teflon filters before measurements to remove the larger size of some TiO_2 nanofibers and the branched macromolecules.

Scanning electron microscopy (SEM) and transmission electron microscopy (TEM) were used to study the morphology. For SEM, the samples were glued to aluminum specimen mounts, and the surface was coated with a mixture of Au and Pd before

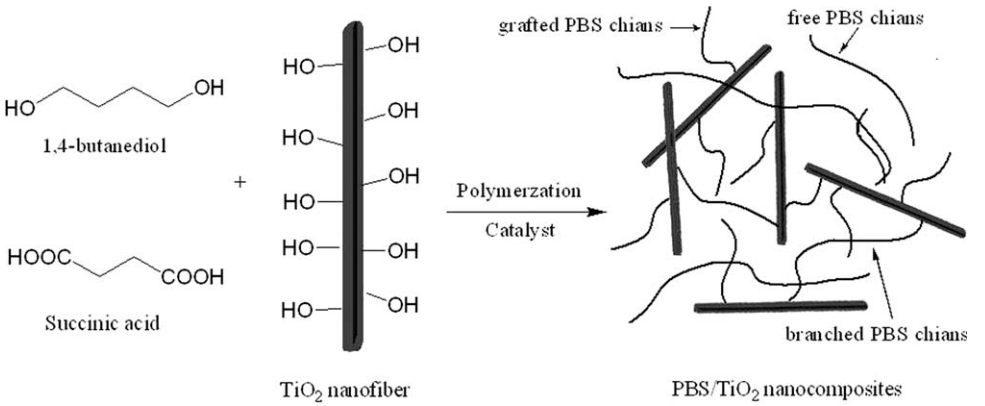

Figure 1. Illustration of the synthesis approach for PBS/TiO_2 nanocomposites.

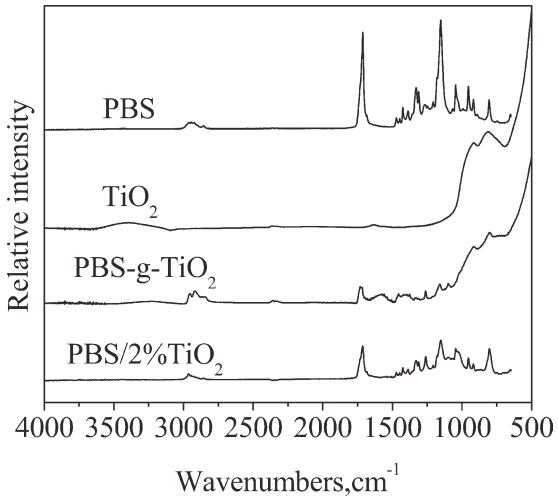

Figure 2. FTIR spectra of PBS, TiO_2 nanofibers, PBS-*g*-TiO_2, and PBS/2%TiO_2.

observation. For TEM, the sample were dissolved in alcohol and ultrasonically treated, then dripping onto copper grids and observed without staining.

Thermal transitions were measured with a Setaram Differential scanning calorimetry (DSC). The sample was conditioned at 150°C for 3 min, cooled to −80°C at a rate of 10°C/min, conditioned at −80°C for 3 min, and then heated again to 150°C at the same rate. The sample was characterized in an inert environment by using nitrogen with a gas flow rate of 50 mL/min.

Decomposition characteristics of the samples were determined with a Pyris1 Thermogravimetric analysis (TGA). About 5 mg of each sample was placed in the pan and heated from 20 to 600°C at rate of 10°C/min under nitrogen atmosphere.

RESULTS AND DISCUSSION

Structure of TiO_2 Nanofibers

The specific surface area determined with a Quadrasorb SI-MP of the TiO_2 nanofibers was 32.4 m^2/g, average pore size was 15.8 nm, and pore volume was 0.083 cm^3/g. XRD indicated that the TiO_2 nanofibers were dominated by anatase crystal structure. The UV spectrum measured on a Carry 5000 indicated that the TiO_2 nanofibers had a strong UV absorption ability at 200–325 nm.

Molecular Weight of PBS/TiO_2

Molecular weight and PDI of pure PBS and PBS/TiO_2 are listed in Table I. The M_n and M_w of pure PBS were 42,300 and 72,700, with PDI of 1.7. While the molecular weight of PBS/0.5%TiO_2, PBS/1%TiO_2, and PBS/2%TiO_2 significantly decreased, with the M_n lowered 25, 35, and 52% than that of pure PBS, respectively. The PDI of PBS/TiO_2 became broader as the adding of TiO_2. Furthermore, the lower viscosities of nanocomposites were observed at the end of polymerization.

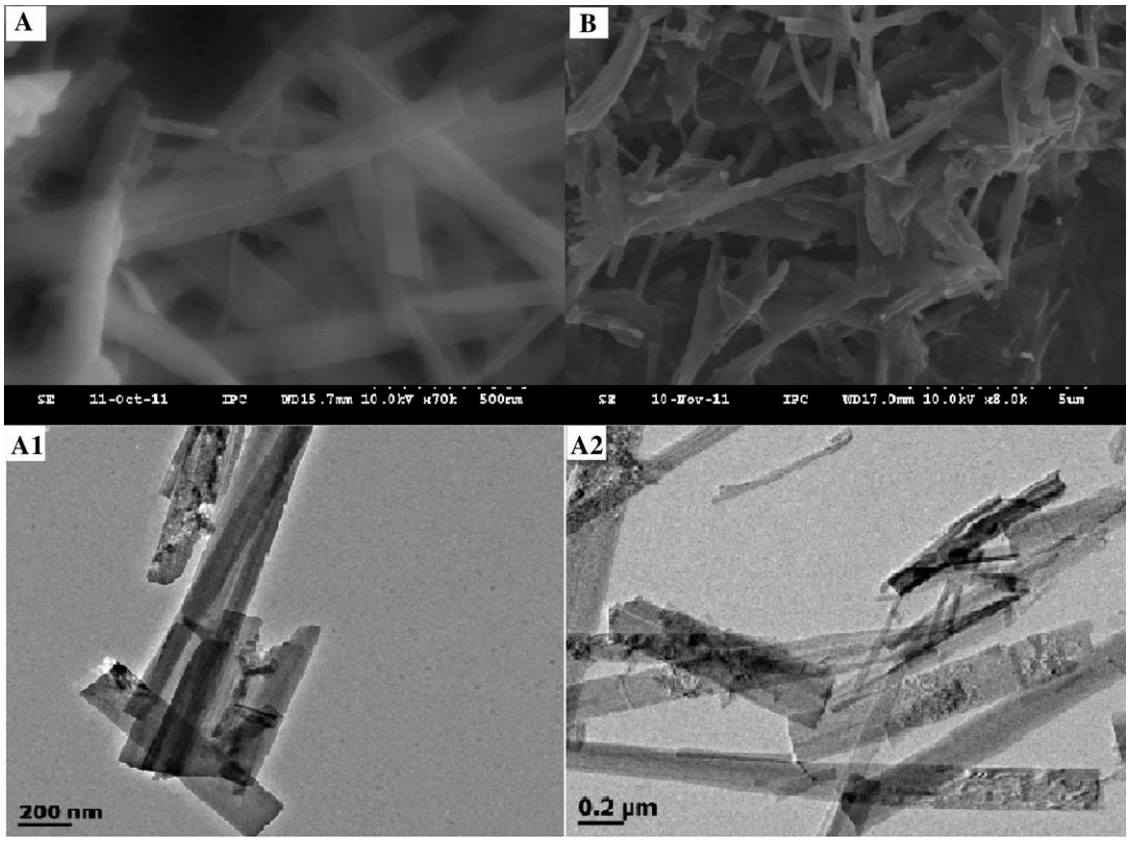

Figure 3. SEM and TEM micrographs of TiO_2 nanofibers (A and B) and PBS-*g*-TiO_2 (A1 and B1).

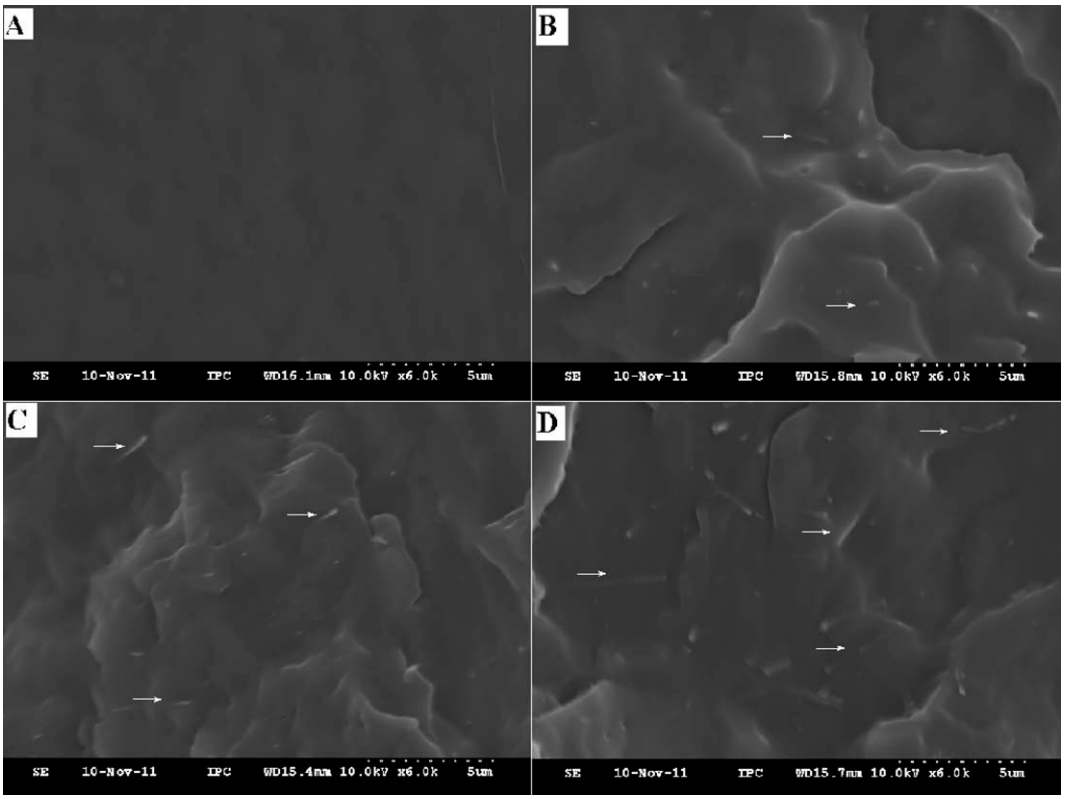

Figure 4. SEM micrographs of the impacted fracture of PBS and PBS/TiO2 (A: PBS; B: PBS/0.5%TiO2; C: PBS/1%TiO2; D: PBS/2%TiO2).

The reason might be the formed of branched structure and filtration of the Teflon filter before GPC measurement. Due to the reactions between TiO_2 surface hydroxyl groups (≡Ti—OH) and carboxyl (—COOH), branched macromolecules were formed, since TiO_2 acted as a multifunctional agent, that lead to the partially reduction of molecular weight and lower intrinsic viscosity (Figure 1). However, the nanocomposites solution was filtered with 0.2 μm Teflon filter before GPC measurement, some macromolecules grafted on TiO_2 could not pass the filter due to the significantly increased size, contributing to the lower molecular weight. In summary, the reactions between TiO_2 and PBS reduced the molecular weight and viscosity of PBS/TiO_2, which was also found *in situ* polymerized nanocomposites of PBS/fumed silica, etc.[27,28]

Chemical Structure of PBS/TiO_2

To confirm the successful grafting of PBS carboxylic group on the TiO_2 nanofibers, the chemical structure of pure PBS, TiO_2 nanofibers, PBS-*g*-TiO_2, and PBS/2%TiO_2 were studied (Figure 2). PBS showed strong C=O stretching band at 1712 cm^{-1}, and C—O stretching band at 1340, 1148, and 1130 cm^{-1}. The asymmetric and symmetric stretching bands of C—H from CH_3 groups of the side chains were observed at 2960 and 2925 cm^{-1}.[29] TiO_2 nanofibers showed bands around 3200 and 1640 cm^{-1}, corresponding to the stretching and bending vibrations of hydroxyl groups on the TiO_2 nanofiber surface. The

Table II. Thermal Properties of PBS and PBS/TiO2 Determined by DSC Thermograms

Samples	T_{cc} (°C)	ΔH_c (J/g)	T_m (°C)	ΔH_m (J/g)	χ_m (%)
PBS	54.8	57.7	114.8	74.6	36
PBS/0.5%TiO_2	59.0	61.4	116.9	88.7	42
PBS/1%TiO_2	64.1	60.0	117.8	80.7	39
PBS/2%TiO_2	69.1	58.2	115.3	75.6	37

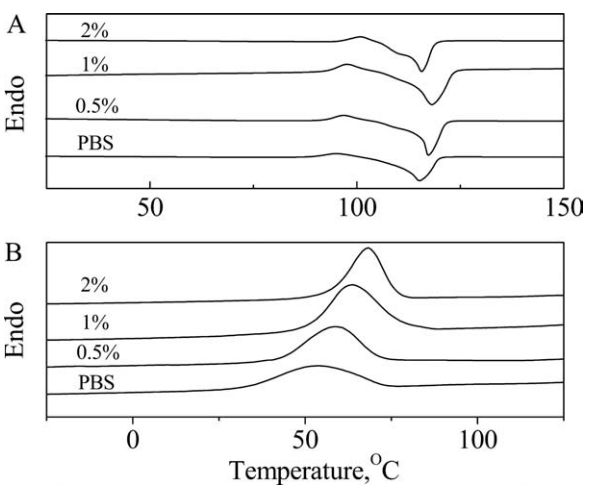

Figure 5. DSC thermograms of PBS and PBS/TiO2 (A: heating process; B: cooling process).

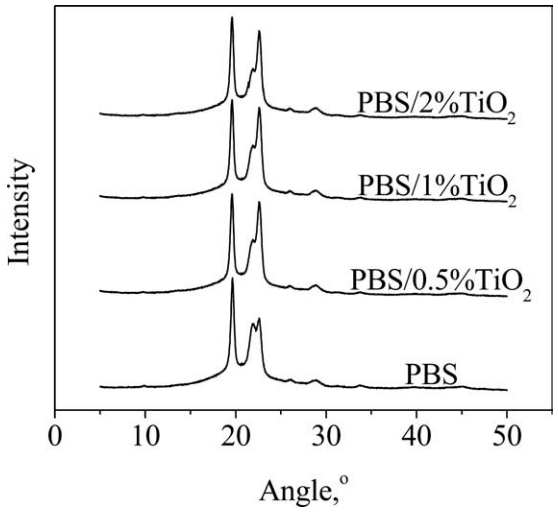

Figure 6. XRD spectrum of PBS and PBS/TiO2.

strong absorption bands between 1000 and 400 cm^{-1} were attributed to the Ti—O and Ti—O—Ti vibrations.[30] In the spectra of PBS-*g*-TiO_2, the bands at 1712, 1340,1148, and 1130 cm^{-1} could be saw, which were caused by the vibrations of C=O and C—O groups from grafted PBS chains. Besides, new bands appeared at 1554 and 1421 cm^{-1} due to the bidentate coordination between Ti and the carboxylic groups of PBS. At last, the PBS/2%TiO_2 showed similar spectra as pure PBS because of the relatively low concentrations of TiO_2 nanofibers.

Morphology

The grafting polymerization between TiO_2 and PBS was further proved by the morphology of TiO_2 nanofibers and PBS-*g*-TiO_2 (Figure 3), which was analogous to the other grafting nanocomposites.[20–22] In SEM, the TiO_2 nanofibers exhibited quite clean and smooth surface, the diameter was 50–100 nm and length was a few microns [Figure 3(A)]. PBS-*g*-TiO_2 seemed much thicker and uncleaner due to the graft of PBS chains, and the nanofibers were fractionally aggregated because of the mutual attraction and the formed of branched structure [Figure 3(A1)]. At higher magnification, TEM further showed differences in morphology between PBS-*g*-TiO_2 and TiO_2 nanofibers, which could further evident the existence of PBS chains on nanofibers surface. The surface of TiO_2 nanofibers seemed almost transparent without any extra phase adhering [Figure 3(B)]. In compared, the PBS-*g*-TiO_2 appeared stained with extra materials that were supposed to come from grafted PBS chains [Figure 3(B1)].

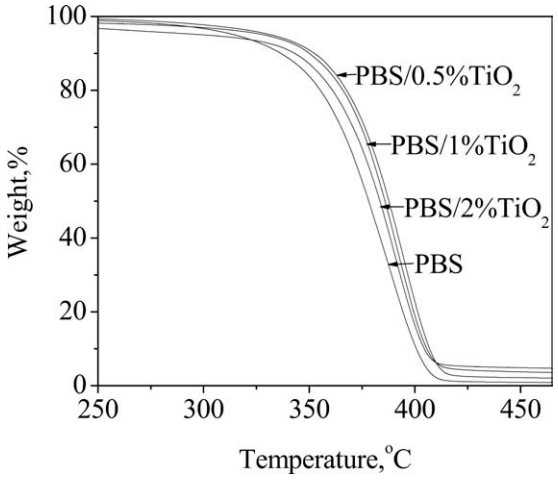

Figure 7. TGA thermograms of PBS and PBS/TiO2 under nitrogen atmosphere.

Table III. Thermal Properties of PBS and PBS/TiO2 Determined by TGA Thermograms

Samples	T_{onset} (°C)	T_{max} (°C)	T_{end} (°C)
PBS	314.8	387.5	420.8
PBS/0.5%TiO_2	332.2	394.7	429.2
PBS/1%TiO_2	339.0	391.1	423.8
PBS/2%TiO_2	340.4	391.1	420.8

In morphology of the nanocomposites, the SEM micrographs of the fractured surface of PBS and PBS/TiO_2 impacted in liquid nitrogen are presented in Figure 4. The fractured surface of pure PBS was quite flat and smooth. As the weight percentage of TiO_2 increased from 0 to 2%, much more coarse and uneven surfaces were observed and the TiO_2 were discernible in the fractured surfaces, which proved the TiO_2 were uniformly distributed into the PBS matrix without the wide range of agglomeration. In short, the ultrasonic treatment and mechanical stirring successfully achieved the good dispersion and compatibility of TiO_2 nanofibers in the PBS matrix that promoted interfacial adhesion between nanofillers and matrix and ultimately influenced the performance of PBS/TiO_2.

Thermal Properties

Cold crystallization temperature (T_{cc}), melting temperature (T_m), heat of melting (ΔH_m), and heat of crystallization (ΔH_c) of PBS and PBS/TiO_2 were determined by DSC and the quantified results are summarized in Table II. The thermograms were obtained from the cooling and heating process after erasing the thermal history, and they exhibited T_{cc} and T_m, respectively (Figure 5). The T_{cc} and T_m of pure PBS was 54.8 and 114.8°C, with crystallinity (χ_m) of 36% ($\chi_m = \Delta H_m/\Delta H^\circ\omega$, where ΔH° = 210 J/g).[31] The raised T_{cc}, T_m, and χ_m were obtained for the PBS/TiO_2, among which T_{cc} of PBS/2%TiO_2 improved 26.2%, T_m of PBS/1%TiO_2 improved 2.6%, and χ_m of PBS/0.5%TiO_2 improved 16.7% compared with pure PBS. The results might be attributed to the combined effects of both the nucleation TiO_2 and PBS-*g*-TiO_2 particles and the forming of branched structure. First, depending on their size and distribution, both TiO_2 and PBS-*g*-TiO_2 acted as nucleating agents and strongly affected nucleation density, spherulite size, and crystallization kinetics as well as brittleness of the PBS matrix, which contributed favorably to the faster rate of the crystallization and χ_m.[32] Second, the branched structure made the process of crystallization

complex that lead to the irregular changes of T_m and χ_m of PBS/TiO_2 with different content of TiO_2.

Besides, the increased χ_m could also be confirmed by the results of XRD (Figure 6). PBS showed three strong diffraction peaks located at 2θ values of 19.6, 21.9, and 22.5°, the three diffraction peaks from small to high angles are assignable to (020), (021), and (110) planes, respectively.[33] The XRD patterns of PBS/TiO_2 had the similar three strong diffraction peaks which had the same angle locations with that of PBS. However, the intensity of the diffraction peaks increased with increasing TiO_2 content, indicating that blending with TiO_2 did modify the crystal structure of PBS but increased the χ_m of PBS in the nanocomposites.

The TGA thermograms are shown in Figure 7, and the decomposition data are summarized in Table III. Pure PBS exhibited a peak decomposition temperature (T_{max}) of 387.5°C and onset (T_{onset}) and end (T_{end}) decomposition temperatures of 314.8 and 420.8°C. The PBS/TiO_2 showed higher thermal stability than that of pure PBS. Specifically, PBS/0.5%TiO_2 had the highest thermal stability and after that amount the stability was slightly decreased, which was in accordance with a recent study that were PBS/SiO_2 nanocomposites.[34] In conclusion, the amount of TiO_2 nanofibers plays an important role to thermal stabilization of PBS that the TiO_2 nanofibers stabilized the decomposition of PBS. This might be explained by the fact that, (1) the concentration of TiO_2 nanofibers could act as a superior insulator and mass transport barrier to the volatile products generated during decomposition, (2) the creation of a tortuous path, resulting by the nanofibers' dispersion into the PBS matrix, slowing the diffusion of the produced substances in the material, and (3) the trend of stabilization was not continuous that should be attributed to the increasing branched macromolecules that exhibited lower thermal stability than the respective linear.[35,36]

CONCLUSIONS

Nanocomposites of PBS/TiO_2 with covalent grafting between TiO_2 nanofibers surface and PBS chains were first synthesized through *in situ* melt polycondensation. With the ultrasonic treatment and mechanical stirring, homogeneous dispersion of TiO_2 nanofibers in the PBS matrix was achieved without obvious agglomeration. The PBS-*g*-TiO_2 nanofibers were isolated and the grafted structure was confirmed by the chemical structure and morphology analysis. As the weight percentage of TiO_2 increased from 0 to 2%, decreased molecular weight was obtained for all the nanocomposites due to the formation of branched macromolecules, among which the M_n of the PBS/2%TiO_2 was 52% lower than pure PBS. To thermal properties and crystallization, the T_{cc}, T_m, χ_m, and thermal stability the PBS/TiO_2 were improved in varying degrees, which were attributed to the combined effects of the nucleation efforts of TiO_2, PBS-*g*-TiO_2 particles and the formation of branched structure. To the thermal stability, the introduction of TiO_2 nanofibers enhanced the thermal stabilization of the nanocomposites, among which PBS/0.5%TiO_2 showed the best result.

REFERENCES

1. Uesaka, T.; Nakane, K.; Maeda, S.; Ogihara, T.; Ogata, N. *Polymer* **2000,** *41*, 8449.
2. Xu, J.; Guo, B. H. *Biotechnol. J.* **2010,** *5*, 1149.
3. Han, S.; Lim, J. S.; Kim, D. K.; Kim, M. N.; Im, S. S. *Polym. Degrad. Stab.* **2008,** *93*, 889.
4. Ray, S. S.; Okamoto, K.; Okamoto, M. *Macromolecules* **2003,** *36*, 2355.
5. Hwang, S. Y.; Eui Sang Yoo, E. S.; Im, S. S. *Polym. Degrad. Stab.* **2009,** *94*, 2163.
6. Shih, Y. F.; Wang, T. Y.; Jeng, R. J.; Wu, J. Y.; Teng, C. C. *J. Polym. Environ.* **2007,** *15*, 151.
7. Shih, Y. F.; Chen, L. S.; Jeng, R. J. *Polymer* **2008,** *49*, 4602.
8. Wang, X.; Yang, H. Y.; Song, L.; Hu, Y.; Xing, W. Y.; Lu, H. D. *Compos. Sci. Technol.* **2011,** *72*, 1.
9. Fujishima, A.; Rao, T. N.; Tryk, D. A. *J. Photochem. Photobiol. C* **2000,** *1*, 1.
10. Al-Abadleh, H. A.; Grassian, V. H. *Surf. Sci. Rep.* **2003,** *52*, 63.
11. Zan, L.; Tian, L.; Liu, Z.; Peng, Z. *Appl. Catal. A* **2004,** *2*, 264.
12. Zan, L.; Wang, S. L.; Fa, W. J.; Hu, Y. H.; Tian, L. H.; Deng, K. J. *Polymer* **2006,** *47*, 8155.
13. Buzarovska, A.; Grozdanov, A.; Avella, M.; Gentile, G.; Errico, M. *J. Appl. Polym. Sci.* **2009,** *114*, 3118.
14. Mirauchi, M.; Li, Y.; Shimizu, H. *Environ. Sci. Technol.* **2008,** *42*, 4551.
15. Li, G. L.; Wang, G. H.; Hong, J. M. *J. Mater. Res.* **1999,** *14*, 3346.
16. Kobayashi, S.; Hanabusa, K.; Hamasaki, N.; Kimura, M.; Shirai, H. *Chem. Mater.* **2000,** *12*, 1523.
17. Zhang, X. Y.; Zhang, L. D.; Chen, W.; Meng, G. W.; Zheng, M. J.; Zhao, L. X. *Chem. Mater.* **2001,** *13*, 2511.
18. Zhang, Y. X.; Li, G. H.; Jin, Y. X.; Zhang, Y.; Zhang, J.; Zhang, L. D. *Chem. Phys. Lett.* **2002,** *365*, 300.
19. Bezrodna, T.; Puchkovska, G.; Shymanovska, V.; Baran, J.; Ratajczak, H. *J. Mol. Struct.* **2004,** *700*, 175.
20. Hojjati, B.; Sui, R.; Charpentier, P. A. *Polymer* **2007,** *48*, 5850.
21. Luo, Y. B.; Wang, X. L.; Xu, D. Y.; Wang, Y. Z. *Appl. Surf. Sci.* **2009,** *255*, 6795.
22. Khaled, S. M.; Sui, R.; Charpentier, P. A.; Rizkalla, A. S. *Langmuir* **2007,** *23*, 3988.
23. Haque, S.; Rehman, I.; Darr, J. A. *Langmuir* **2007,** *23*, 6671.
24. Jordan, J.; Jacob, K. I.; Tannenbaum, R.; Sharaf, M. A.; Jasiuk, I. *Mater. Sci. Eng.* **2005,** *1*, 393.
25. Yang, D. J.; Liu, H. W.; Zheng, Z. F.; Yuan, Y.; Zhao, J. C.; Waclawik, E. R.; Ke, X. B.; Zhu, H. Y. *J. Am. Chem. Sci.* **2009,** *131*, 17885.
26. Li, Y. H.; Chen, C. H.; Li, J.; Sun, X. S. *Polymer* **2011,** *52*, 2367.

27. Vassiliou, A. A.; Bikiaris D.; Mabrouk, K. E.; Kontopoulou, M. *J. Appl. Polym. Sci.* **2011,** *119*, 2010.
28. Choi, Y. S.; Choi, M. H.; Wang, K. H.; Kim, S. O.; Kim, Y. K.; Chung, I. J. *Macromolecules* **2001,** *34*, 8978.
29. Coutinho, D. F.; Pashkuleva, I. H.; Alves, C. M.; Marques, A. P.; Neves, N. M.; Reis, R. L. *Biomacromolecules* **2008,** *9*, 1139.
30. Bezrodna, T.; Puchkovska, G.; Shimanovska, V.; Chashechnikova, I.; Khalyavka, T.; Baran J. *Appl Surf. Sci.* **2003,** *214*, 222.
31. George Z. P.; Dimitris N. B. *Polymer* **2005,** *46*, 12081.
32. Qian, J.; Zhu, L.; Zhang, J.; Whitehouse, R. *J. Polym. Sci. Part B: Polym. Phys.* **2007,** *45*, 1564.
33. Ihn, K. J.; Yoo, E. S.; Im, S. S. *Macromolecules* **1995,** *28*, 2460.
34. Vassiliou, A. A.; Chrissafis, K.; Bikiaris, D. N. *Thermochim. Acta* **2009,** *495*, 120.
35. Chrissafis, K.; Bikiaris, D. *Thermochim. Acta* **2011,** *523*, 1.
36. Bikiaris, D. *Thermochim. Acta* **2011,** *523*, 25.